Supporting material

Multiplexed single-cell analysis of fine needle aspirates allows accurate diagnosis of salivary gland tumors

Juhyun Oh[1,2], Tae Yeon Yoo[3], Talia M. Saal[1], Lisa Tsay[1], William C. Faquin[4], Jonathan C.T. Carlson[1,5], Daniel G. Deschler [6,7], Sara I. Pai[1,5,8*], Ralph Weissleder[1,2,3,5*]

[1] Center for Systems Biology, Massachusetts General Hospital, 185 Cambridge St, CPZN 5206, Boston, MA 02114

[2] Department of Radiology, Massachusetts General Hospital and Harvard Medical School, Boston, MA 02114

[3] Department of Systems Biology, Harvard Medical School, 200 Longwood Ave, Boston, MA 02115

[4] Department of Pathology, Massachusetts General Hospital and Harvard Medical School, Boston, MA 02114

[5] MGH Cancer Center, Massachusetts General Hospital and Harvard Medical School, Boston, MA 02114

[6] Department of Otolaryngology, Massachusetts Eye and Ear Infirmary, Boston, MA 02114

[7] Department of Otology and Laryngology, Harvard Medical School, Boston, MA 02114

[8] Department of Surgery, Massachusetts General Hospital and Harvard Medical School, Boston, MA 02114

*Corresponding authors:
R. Weissleder, MD, PhD (contact)
S. I. Pai, MD, PhD,
Center for Systems Biology
Massachusetts General Hospital
185 Cambridge St, CPZN 5206
Boston, MA, 02114
617-726-8226
rweissleder@mgh.harvard.edu

Supporting Figure 1. Sample processing of FNA samples. A. FNA samples were obtained *ex vivo* using 22G needle on surgically removed tumor tissue. B. Cells in each FNA sample were cytocentrifuged by Cytospin and then attached on a glass slide. C. Cells were imaged on the glass slide. An example image of H&E stain of an FNA sample (salivary duct carcinoma) is presented on the right.

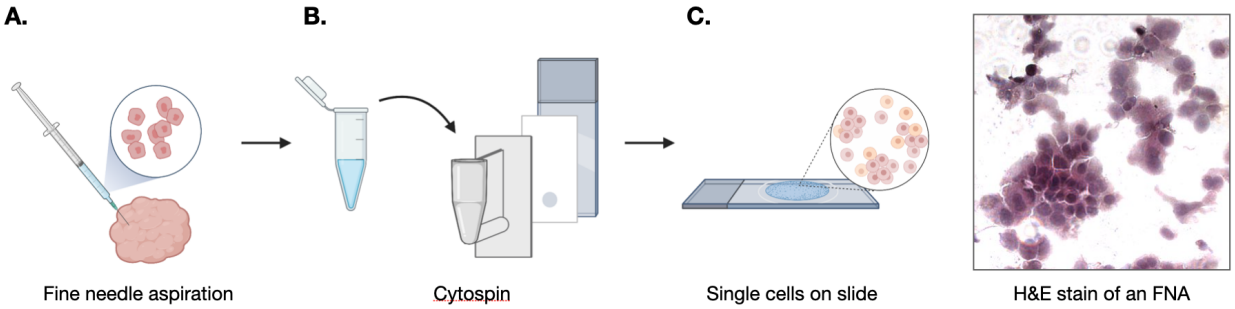

Supporting Figure 2. Overview of the chemistry enabling FAST imaging. The FAST linker synthesis starts with a lysine scaffold contains a PEG_4 linker for efficient antibody conjugation: i. TSTU, DIPEA; ii. H_2N-PEG_4-CO_2H; iii. DCM/TFA (20%); iv. rTCO-PNP, DIPEA; v. piperidine (7.5%). The linker was functionalized with AF488, AF555 or AF647. To generate the quencher, BHQ3-amine was coupled with HTz-PEG_5-NHS to yield BHQ3-Tz in one step. The fluorescent signal of FAST-labeled antibodies can be efficiently quenched (>90%) with 10 µM of BHQ3-Tz in < 1 min[8].

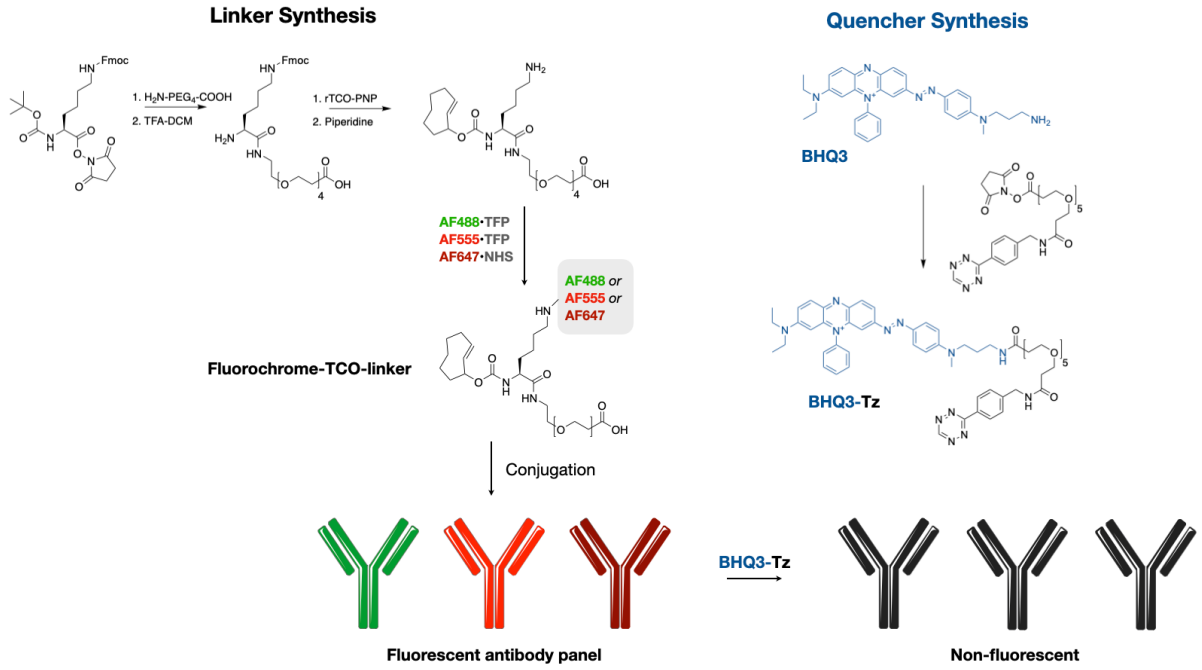

Supporting Figure 3. Validation of antibody specificity and biomarker expression across samples. To compare the FAST-FFPE staining to immunohistochemistry, we processed a number of FFPE sections of representative samples for both methods. Shown here is one example of mucoepidermoid carcinoma cases, expressing high levels of CK7, MUC1, p63. The staining patterns matched between FAST-FFPE and IHC. Reproducible staining patterns of the FAST antibodies were observed across multiple sections.

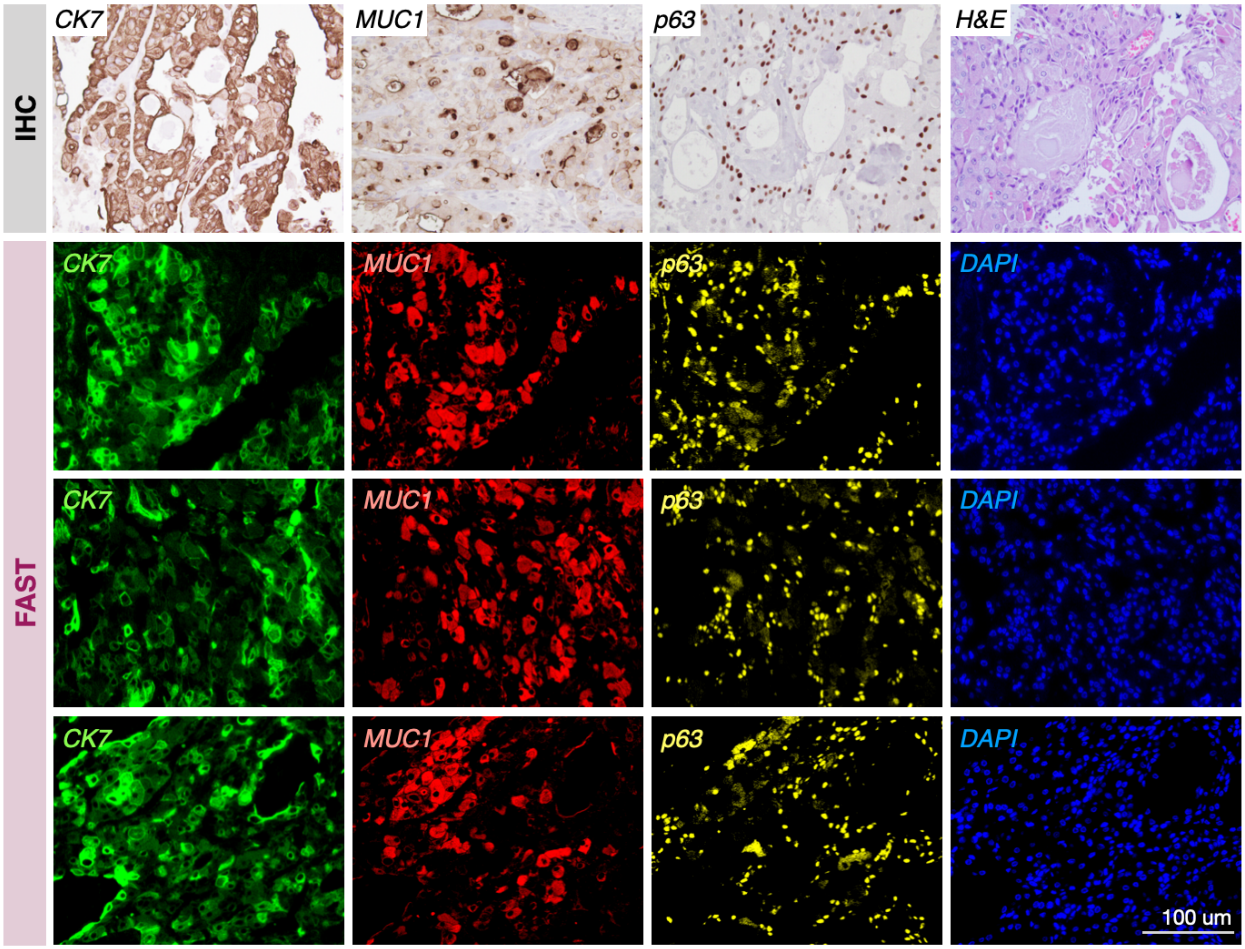

Supporting Figure 4. Biomarker detection in FFPE tissue sections of different SGT subtypes. To assess and compare the expression pattern and level of each biomarker measured by FAST antibody staining in FNA and tissue sections, FFPE tissue sections of representative samples for each subtype were imaged (PA, MuEC, LEC, and MyEC are shown). High expression of key molecular markers in each SGT subtypes was detected matching with the results from FAST-FNA (**Fig.2**).

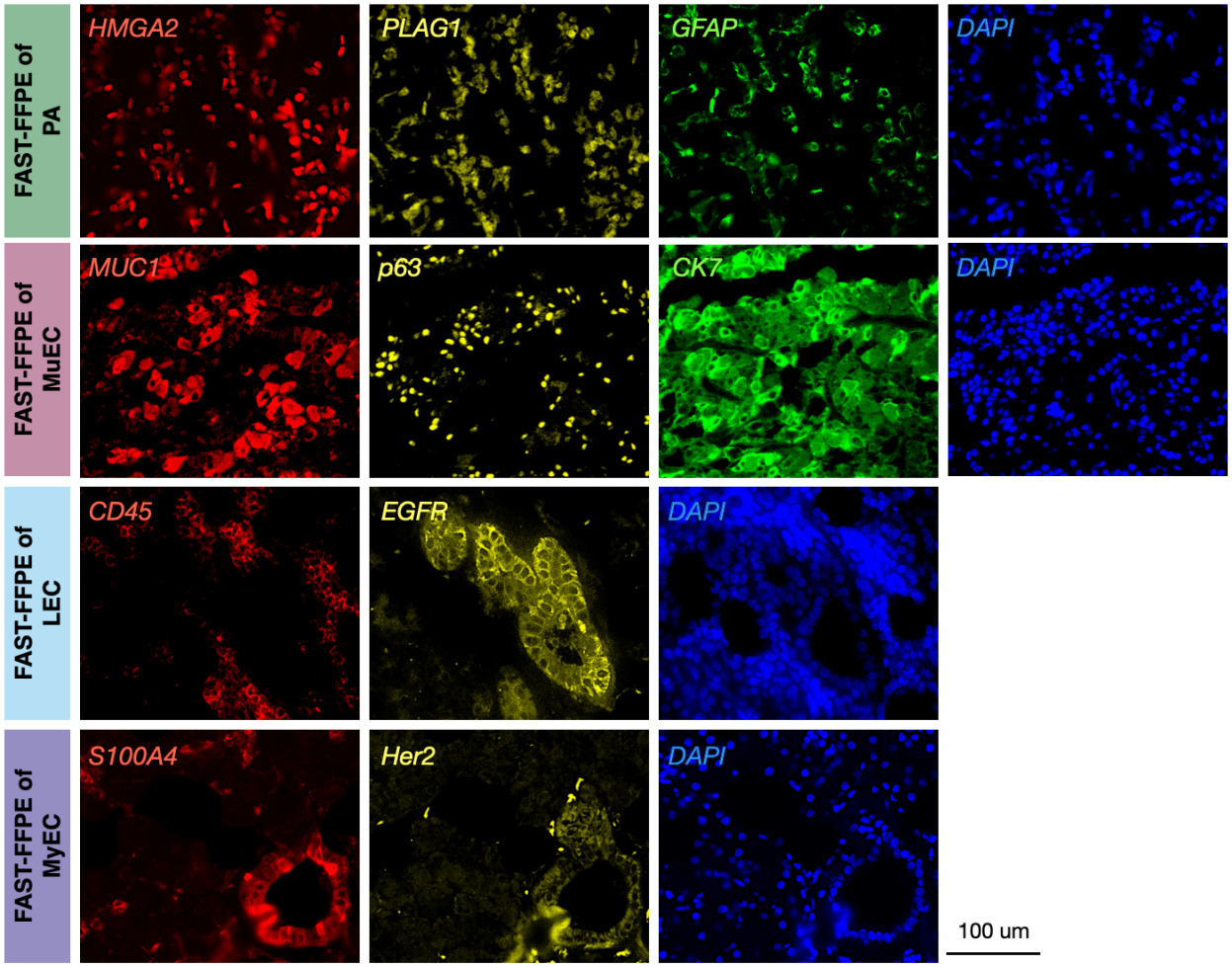

Supporting Figure 5. Normalization and global threshold setting strategy. Normalization was necessary to account for the the multiplicative batch effect in the fluorescent intensities measured in individual cells imaged for a given marker (EPCAM in this example). Samples were first normalized to the 10th percentile of signal to align the left edge of negative peak in each sample. Aligned data was combined for each marker to set the global threshold for the positive signal. Threshold was placed at the full width at half maximum (FWHM) away from the peak location of negative peak of the aggregate data.

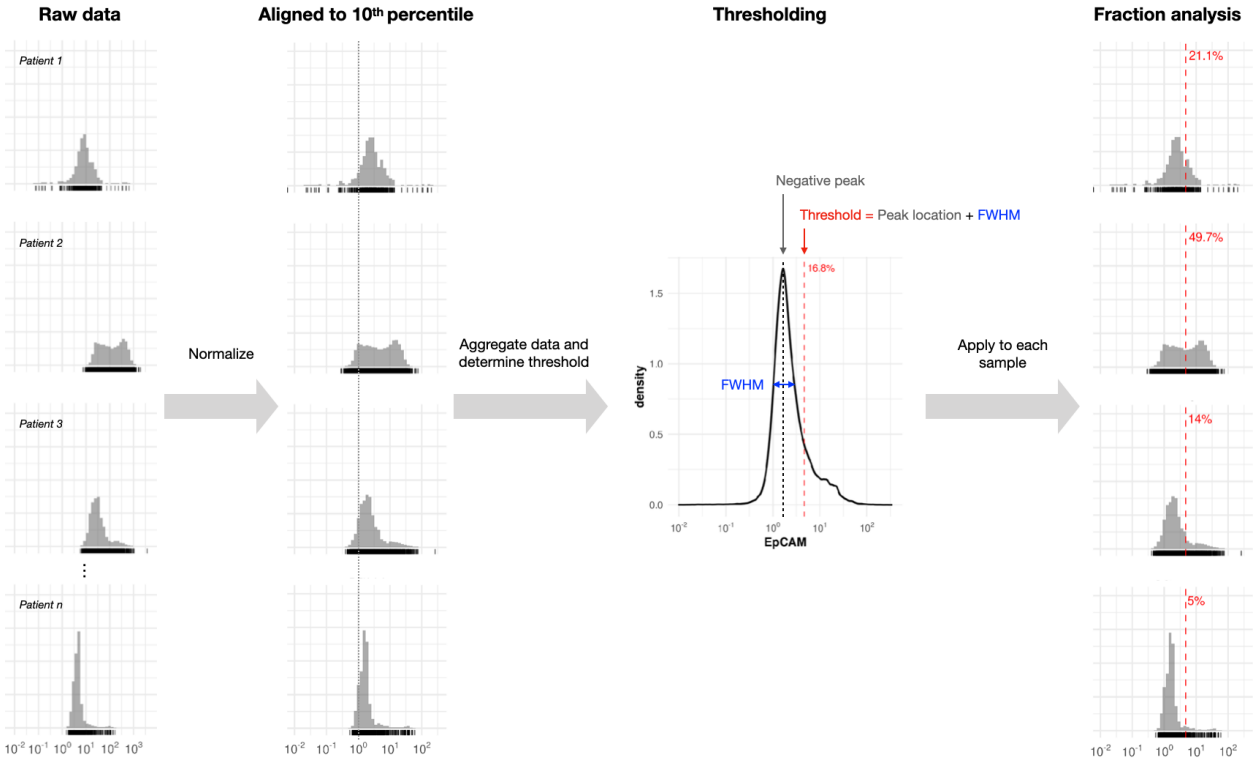

Supporting Figure 6. ROC curves of PA diagnosis based on HMGA2, GFAP, or PLAG1. A. The positive fraction of HMGA2, GFAP, or PLAG1 expressing cells in each specimen of both PA and non-PA cases was used for ROC plots. The threshold was determined at the fraction value that maximizes the sum of sensitivity and specificity as shown in each table. Accuracy was calculated as the ratio of correctly identified specimens in all PA and non-PA samples included in the analysis. **B.**The positive fraction of each marker in PA and non-PA specimens are shown for comparison. Student's t-test was used for statistical analysis.

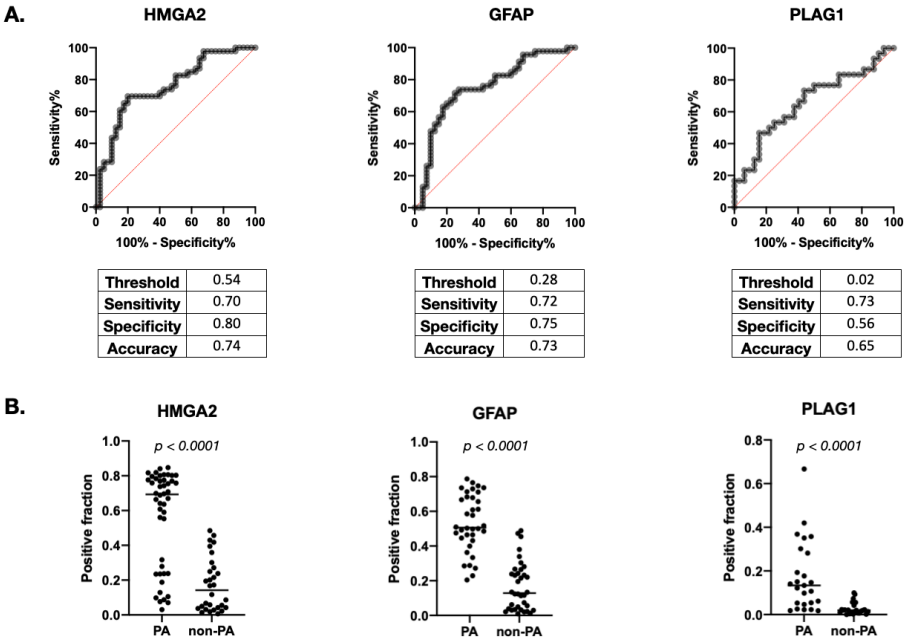

Supporting Figure 7. Correlation between analysis results of single cell homogenate of tissues and its FNA. To validate FAST-FNA measurements, we performed a direct comparison between the results from single cell homogenate of surgically removed SGT tissues and its FNA samples obtained post-operatively. Bar graphs present the fraction of positively stained cells for each marker. In general there were good correlations between the two sample types, and the biomarker expression profiles were similar. Overall, the average Pearson correlation coefficient was ρ=0.89 with standard deviation of 0.02.

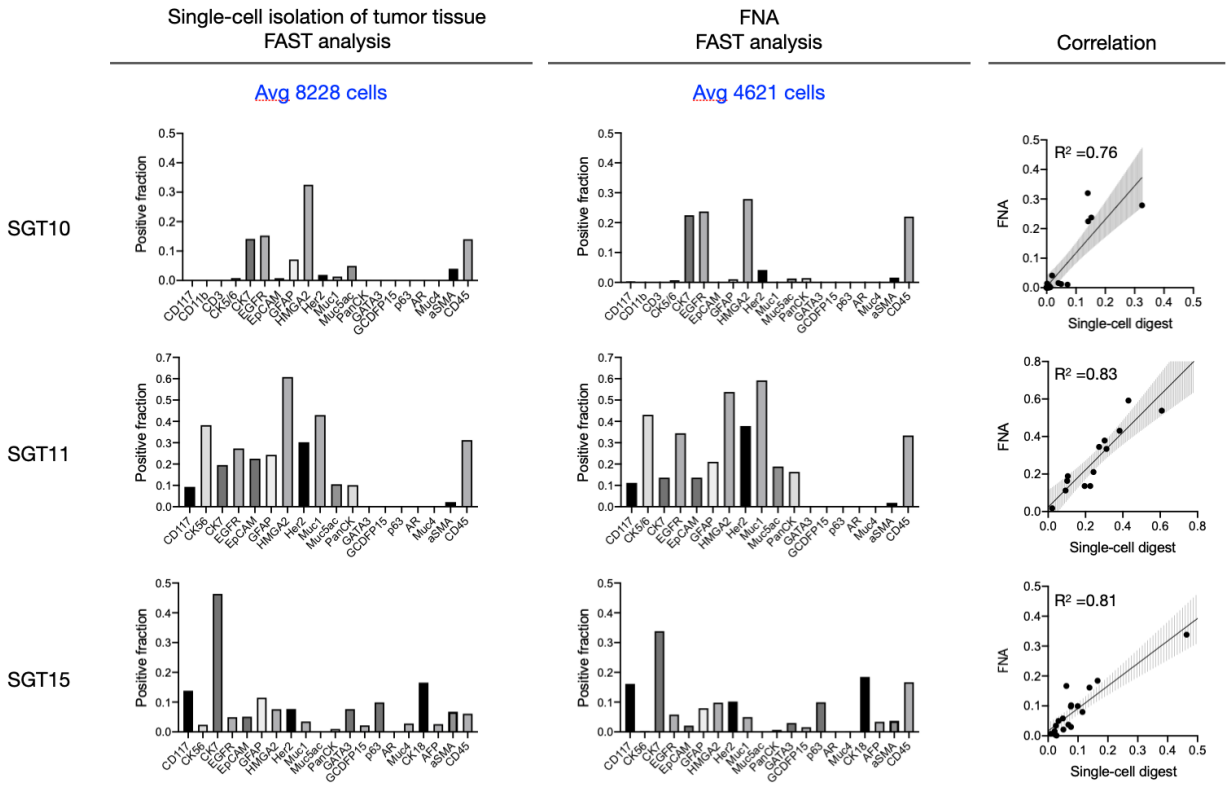

Supporting Figure 8. Correlation of nuclear NTRK measurement by FAST-FFPE and IHC. The fluorescent intensity of NTRK stain in FFPE tissue sections imaged by FAST-labeled antibody (FAST-FFPE) was compared to the signal intensity measured by IHC in consecutive sections. Each datapoint represents the signal measured in individual cells in representative tissue sections of FFPE and IHC. Signal intensity was measured after background subtraction and scaling to 1 as maximum value. The Pearson correlation coefficient was ρ=0.70.

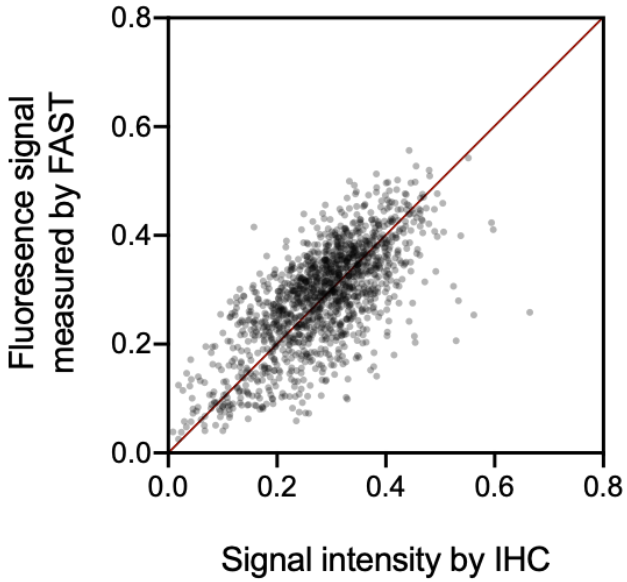

Supporting Figure 9. Summary of SGT specimen processing for various analyses presented in the study.

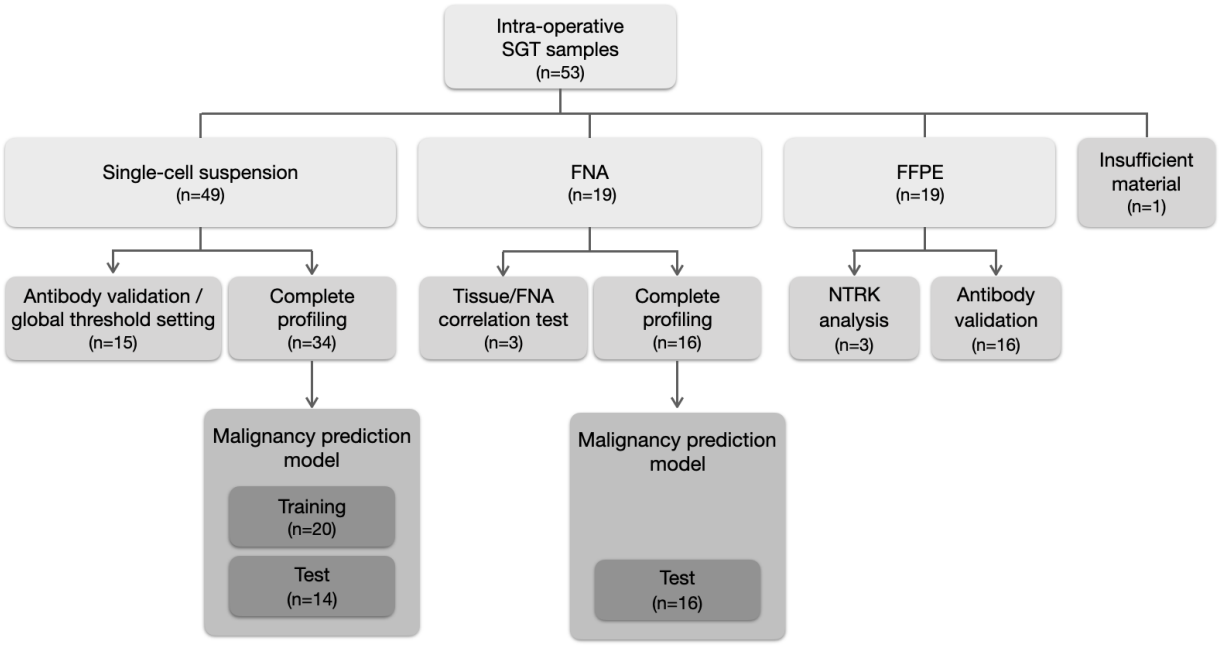

Supporting Table 1. Antibodies utilized for FAST imaging to characterize various SGT subtypes. Additional information is included in **Supporting Table 2**.

	Marker	Target	Vendor	Cat #	Clone	Isotype
1	p63	MuEC, MyEC	Abcam	ab735	4A4	Mouse IgG2a
2	NTRK	SC	Abcam	ab76291	EP1058Y	Rabbit IgG
3	CD45	Immune cells	BD Pharmingen	555480	Hi30	Mouse IgG1
4	EpCAM	Tumor cells	Biolegend	324202	9C4	Mouse IgG2b
5	EGFR	Tumor cells	Selleck Chemicals	A2000	-	Human IgG1
6	Her2	SDC	BioXcell	BE0277	7.16.4	Mouse IgG2a
7	Muc1	MuEC	Fitzgerald	10-M93A	M01102909	Mouse IgG
8	CK5/6	MyEC,MuEC	Millipore	MAB1620	D5/16B4	Mouse IgG1
9	Muc4	MuEC	ThermoFisher	35-4900	1G8	Mouse IgG1
1	AFP	Tumor cells	Biolegend	847102	BSB-23	Mouse IgG2a
1	CD117	AdCC	Biolegend	313202	104D2	Mouse IgG1
1	LEF1	BCA	R&D	AF7647	Polyclonal	Goat IgG
1	GATA3	SC,SDC	BD Biosciences	558686	L50-823	Mouse IgG1
1	GCDFP15	SC	Biolegend	915106	D6	Mouse IgG2a
1	CK18	Tumor cells	Biolegend	628401	DA-7	Mouse IgG1
1	AR	SDC	CST	5153	D6F11	Rabbit IgG
1	GFAP	PA	Biolegend	644702	2E1.E9	Mouse IgG2b
1	CK7	MuEC,SDC,AdC	Biolegend	601601	W16155A	Rat IgG2a
1	TrkB	SC	R&D	MAB3971	72509	Mouse IgG1
2	HMGA2	PA	CST	8179S	D1A7	Rabbit IgG
2	Myb	AdCC	R&D	AF6209	Polyclonal	Sheep IgG
2	NR4A3	ACC	Mlilipore sigma	HPA043360	Polyclonal	Rabbit IgG
2	s100A4	SC, MyEC	Biolegend	810101	S100A4	Rabbit IgG
2	TrkC	SC	R&D	AF373	Polyclonal	Goat IgG
2	PLAG1	PA	Novus Biologicals	H00005324-M02	3B7	Mouse IgG2a
2	Sox10	ACC, MyEC	R&D	AF2864	Polyclonal	Goat IgG
2	Muc5ac	MuEC	ThermoFisher	MA5-12175	45M1	Mouse IgG1
2	aSMA	Fibroblasts	ThermoFisher	14-9760-80	1A4	Mouse IgG2a
2	panCK	MuEC, ACC	Biolegend	914204	AE-1/AE-3	Mouse IgG1
3	Rabbit IgG	2' for NTRK	Biolegend	410404	6B9G9	Mouse IgG1
3	Isotype control	N/A	BioXcell	BE0083	MOPC-21	Mouse IgG1
3	Isotype control	N/A	BioXcell	BE0085	C1.18.4	Mouse IgG2a
3	Isotype control	N/A	BioXcell	BE0086	MPC-11	Mouse IgG2b
3	Isotype control	N/A	Biolegend	910801	Poly29108	Rabbit IgG
3	Isotype control	N/A	R&D	AB-108-C	Polyclonal	Goat IgG
3	Isotype control	N/A	R&D	5-001-A	Polyclonal	Sheep IgG
3	Isotype control	N/A	BioXcell	BE0089	2A3	Rat IgG2a

Tumor subtype abbreviations: MyEC, myoepitheliam carcinoma; MuEC, mucoepidermoid carcinoma; SC, secretory carcinoma; SDC, salivary duct carcinoma; ACC, acinic cell carcinoma; AdCC, adenoid cystic carcinoma; PA, pleomorphic adenoma; BCA, basal cell adenoma.

Supporting Table 2. Biomarkers commonly used in SGT subtype analysis and the cell lines used for antibody testing of each biomarker.

Marker	Target	Pattern	Reference	Cell line
NR4A3	ACC	N	*Am J Surg Patho, 2019; 43(9):1264-72*	A431
SOX10	ACC, MyEC	N	*Int J Mol Sci, 2021;22:6776*	U-2 OS
CD117	AdCC	M/C	*Int J Mol Sci, 2021;22:6776*	HEK293
MYB	AdCC	N	*Int J Mol Sci, 2021;22:6776*	THP-1
LEF1	BCA	N	*Diagn Cytopathol, 2017;45(12):1078-83*	HEK293
TP63	MuEC	N	*Int J Mol Sci, 2021;22:6772*	RT4
MUC1	MuEC	C	*Int J Mol Sci, 2021;22:6772*	U-2 OS
MUC4	MuEC	C	*Int J Mol Sci, 2021;22:6772*	MCF-7
MUC5AC	MuEC	C	*Int J Mol Sci, 2021;22:6772*	A549
GFAP	PA	C	*Int. J. Mol. Sci. 2021, 22(13), 6771*	U-2 OS
HMGA2	PA	N	*Genes Chromosom Cancer 2009;48(1):69-82*	A431, U-2 OS
PLAG1	PA	N	*Int J Mol Sci, 2021;22:6776*	U-2 OS
panNTRK	SC	N/C	*Histopathology, 2019;75(1):54-62*	CAPAN-2
GCDFP15	SC,SDC	C	*Am J Surg Patho, 2010; 34(5)599-608*	MDA-MB231
TRKB	SC	C	*Ann Diagn Pathol, 2021; 50(9):151673*	U-2 OS
S100	SC,MyEC	C	*Am J Surg Patho, 2010; 34(5)599-608*	A549
TRKC	SC	N	*Oncogene 2013; 32,3698–3710 (2013)*	A549, U-2 OS
GATA3	SC,SDC	N	*Head and Neck Pathol. 2013;7(4):311-5*	A431, U-2 OS
AR	SDC	N/C	*Int J Cancer, 2018;143(4):758-766*	U-2 OS
EpCAM	Tumor cells	M	*Arch Oral Biol. 2017;79:87-94; Pathology 2018; 50(7)*	A431
EGFR	Tumor cells	M	*Oral Oncol, 2012; 48(10):991-996*	A431
HER2	SDC	C/M	*Diagn Histopathol, 2020; 26(4): 159-164*	BT474
CK5/6	MyEC,MuEC	C	*Int J Mol Sci, 2021;22:6771*	A431
AFP	Tumor cells	C	*J Nihon Univ Sch Dent, 1992; 34:240-248*	MCF-7
CK18	Tumor cells	C	*J Oral Biol Craniofac Res. 2014; 4(2): 127–134*	A431, U-2 OS
CK7	MuEC,SDC,AdCC	C	*Int J Mol Sci, 2021;22:6771*	RT4
panCK	MuEC, ACC	C	*Int J Mol Sci, 2021;22:6771*	MCF-7
SMA	Fibroblasts	C	*Front Biosci. 2010;15:226–236*	A431
CD45	Immune cells	M	*Annu Rev Immunol, 1994; 12, 85–116*	PBMC

Tumor subtype abbreviations: MyEC, myoepitheliam carcinoma; MuEC, mucoepidermoid carcinoma; SC, secretory carcinoma; SDC, salivary duct carcinoma; ACC, acinic cell carcinoma; AdCC, adenoid cystic carcinoma; PA, pleomorphic adenoma; BCA, basal cell adenoma. **Protein expression pattern**: N, nucleus; C, cytosol; M, membrane. The Cell line column includes cell lines expressing a putative marker (The Human Protein Atlas: https://www.proteinatlas.org) that was used for initial antibody validation.

Supporting Table 3. Cost estimate.

Items		Unit price ($/unit)	Cost per sample ($)
Antibody conjugation		11.37 per antibody (10 ul reaction)	0.57
Glass slide		0.62 each slide	0.62
Octospot		2.14 each slide	2.14
Antibodies	anti-p63	2.10 / µl	0.53
	anti-NTRK	8.57 / µg	2.14
	anti-CD45	0.84 / µg	0.21
	anti-EpCAM	1.75 / µg	0.44
	anti-EGFR	0.14 / µg	0.04
	anti-Her2	0.15 / µg	0.04
	anti-Muc1	0.25 / µg	0.06
	anti-CK5/6	0.29 / µg	0.07
	anti-Muc4	3.98 / µg	0.99
	anti-AFP	2.95 / µg	0.74
	anti-CD117	1.50 / µg	0.38
	anti-LEF1	4.36 / µg	1.09
	anti-GATA3	3.48 / µg	0.87
	anti-GCDFP15	1.95 / µg	0.49
	anti-CK18	1.85 / µg	0.46
	anti-AR	5.51 / µg	1.38
	anti-GFAP	2.50 / µg	0.63
	anti-CK7	2.15 / µg	0.54
	anti-TrkB	5.16 / µg	1.29
	anti-HMGA2	4.89 / µg	1.22
	anti-Myb	4.76 / µg	1.19
	anti-NR4A3	7.16 / µl	1.79
	anti-s100A4	1.95 / µg	0.49
	anti-TrkC	5.16 / µg	1.29
	anti-PLAG1	8.58 / µg	2.15
	anti-Sox10	5.40 / µg	1.35
	anti-Muc5ac	4.04 / µg	1.01
	anti-aSMA	4.20 / µg	1.05
	anti-panCK	1.95 / µg	0.49
	anti-Rabbit IgG	2.75 / µg	0.69
	Mouse IgG1 isotype	0.15 / µg	0.04
	Mouse IgG2a isotype	0.15 / µg	0.04
	Mouse IgG2b isotype	0.15 / µg	0.04
	Rabbit IgG isotype	1.82 / µg	0.46
	Goat IgG isotype	0.11 / µg	0.03

	Sheep IgG isotype	0.11 / µg	0.03
	Rat IgG2a isotype	0.15 / µg	0.04
Total			**29.12**